Cellulose (2022) 29:1911–1928
https://doi.org/10.1007/s10570-021-04388-3

ORIGINAL RESEARCH

Novel functionalized cellulose derivatives fabricated with Cu nanoparticles: synthesis, characterization and degradation of organic pollutants

Faiza Lughmani · Farzana Nazir · Shahid Ali Khan · Mudassir Iqbal

Received: 8 April 2021 / Accepted: 17 December 2021 / Published online: 11 January 2022

Abstract In this study, microcrystalline cellulose (MCC) was modified to oxidized cellulose (OC), 6-deoxycellulose hydrazide and 6-deoxycellulose (N,N-diethyl)amine (MCC-Hyd and MCC-DEM) derivatives and employed as supporting material for the synthesis of copper nanoparticles (NPs). Copper ions from aqueous solution were adsorbed and then reduced to zero valent copper (ZVC) NPs using sodium borohydride on films of prepared derivatives. The characterization of prepared derivatives and Cu NPs embedded films was performed using Fourier Transform Infrared Spectroscopy, Elemental analysis, X-ray diffraction, Scanning Electron Microscopy, X-ray photoelectron spectroscopy and Nuclear Magnetic Resonance spectroscopy. Ultraviolet/Visible (UV–VIS) spectroscopy was performed for the degradation studies of 4-nitrophenol (4-NP) and various azo dyes viz. Congo Red, Methylene Blue, and Methyl orange. Results revealed that all the films showed degradation only in the presence of ZVC NPs. Oxidized cellulose, MCC-Hyd and MCC-DEM showed excellent degradation efficiencies (> 85%) in all the cases. Our findings revealed that MCC derivatives could be efficient and renewable candidates for removal of water pollutants in future.

Supplementary Information The online version contains supplementary material available at https://doi.org/10.1007/s10570-021-04388-3.

F. Lughmani · F. Nazir · M. Iqbal (✉)
Department of Chemistry, School of Natural Sciences, National University of Science and Technology (NUST), Islamabad 44000, Pakistan
e-mail: mudassir.iqbal@sns.nust.edu.pk

S. A. Khan
Department of Chemistry, University of Swabi, Swabi Anbar, Khyber Pakhtunkhwa 23561, Pakistan

Graphical abstract

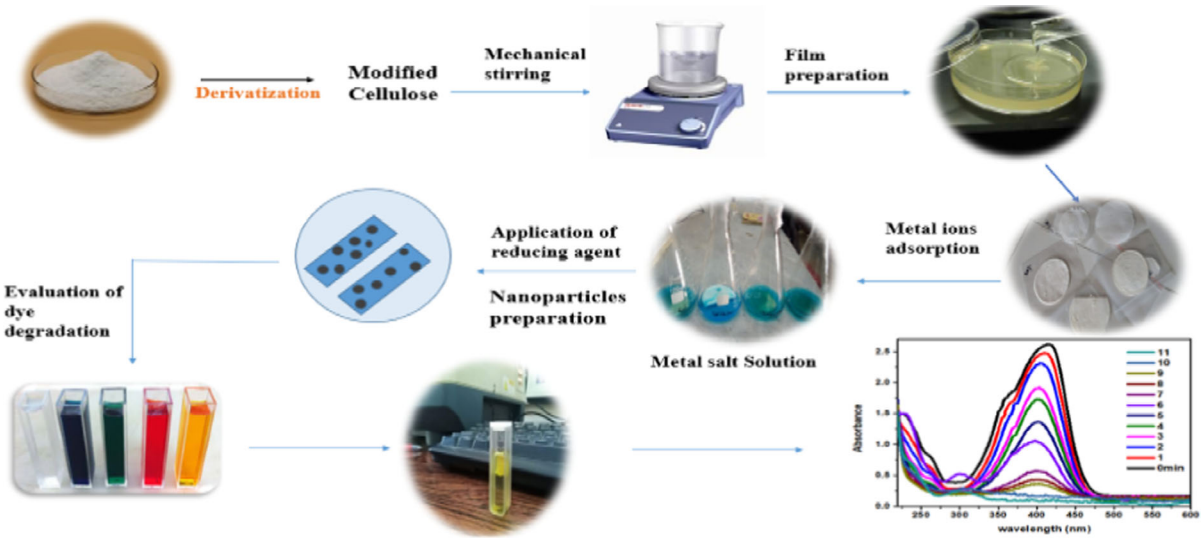

Keywords Cellulose derivatives · Cu nanoparticles · Degradation · Organic pollutants

Introduction

Pollution in its all form, is a severe menace to the human health (Ali, Kamal et al. 2018).Water pollution causes diarrhea, cholera, malaria, dengue, typhoid, kidney damage, cancer, loss of life in extreme cases (Haines et al. 2006) (Raaschou-Nielsen et al. 2013), and tuberculosis etc. Industries like textile, plastics and pigments, pharmaceuticals, and cosmetics are extensively taking advantage of phenolic compounds and dyes for coloring purposes. Colored effluent from these industries is taken as a momentous source of environmental contamination (Sha et al. 2016; Yousef et al. 2016). More than 100,000 commercially available dyes are extensively utilized by these industries. Annual production of synthetic dyes worldwide is over 0.7 million tons (Spadaro et al. 1994; Robinson et al. 2001; Amoozegar et al. 2011). Approx. 15% of dye is lost in the course of dyeing process and is released unprocessed to the environment in the form of industrial waste (Robinson et al. 2001; Parshetti et al. 2010), which has serious effects on color and quality of water. It also affects the human health as well as aquatic life. Owing to the scenario cited above, it has become highly mandatory to remove these dyes and pesticides from wastewater to avoid unwanted serious consequences.

Therefore, effective strategies are required for the treatment of organic waste in order to eradicate, or at least minimize the quantity of toxic substances from wastewater. Various techniques presently being employed to eliminate colored chemicals and hazardous metals are electrochemical treatment, filtration, precipitation, osmosis, flotation, coagulation, flocculation, and adsorption (Dabrowski, Hubicki et al. 2004, Chen et al. 2009; Min et al. 2012; Pal et al. 2015; Razali et al. 2015; Teh et al. 2016). The major hindrance in attaining the achievement of physical methods is the limitations coupled with, such as possibility of secondary pollutants formation, high cost and partial treatment. Hence there is a dire need to focus on the development of methods that may completely deteriorate organic pollutants, especially with the assistance of an efficient catalyst.

Applications of metallic nanoparticles in various areas have gained growing attention in recent times. These includes sensing, drug delivery, bio-imaging and antibacterial coating (Ismail, Gul et al. 2019). They have also been employed in different reactions involving coupling, electrochemical, and oxidation and reduction reactions (Wang and Gu 2015). Metallic

nanoparticles are widely employed catalysts for the degradation of organic pollutants, because of larger surface area, catalytic efficiency, easy production, and selectivity for reactions.

However, the low stability of most abundantly available metallic nanoparticles restricts the actual environmental applications in contrast to noble metals which exhibit more stable nanoparticles. For example, nickel nanoparticles are highly susceptible to air and under ordinary circumstances are quickly oxidized, that may restrict their practical applications. (Yang et al. 2013; Kamal et al. 2016a, b; Wang et al. 2017). Other problems associated with use of nanoparticles are agglomeration and separation. Because of extremely small size, it is very difficult to separate these from reaction mixture. Agglomeration occurs because of van der Waals interactions, causing reduction of surface area and resulting in decreases of catalytic efficiency (Kamal et al. 2016a, b). Therefore, to overcome these limitations, we need an adequate support material to achieve an effective catalytic activity (Haider et al. 2016). These supporting materials may reduce the efficiency to some extent, as a consequence of their relatively small surface area, which ultimately leads to poor accessibility of catalyst towards the reacting species (Guo, Liang et al. 2007, Zhou et al. 2013).

So active and compelling materials are desired to bring about stability, easy separation, enhanced catalytic activity and reusability (Shokouhimehr 2015; Bakhsh et al. 2018; Khan et al. 2019). As per literature, polymer hybrids and composites are the materials being extensively used to support metallic nanoparticles. e.g. copper nanoparticles incorporated on chitosan-coated cellulose microfiber mats (CS-CMM) as catalyst were employed for the reduction studies of 4NP, 2NP and cresyl blue dye (Haider et al. 2016). Reduction of thymol violet using TiO_2/Cs-CMM catalyst was also carried out, reaction equilibrium was attained in 90 min (Kamal et al. 2016a, b). Au nanoparticles embedded in poly(AMPS-co-HEMA) composites were used for selective reduction of nitrophenols and reduction occurred in 20 min (Wang et al. 2012). Cellulose acetate fibers loaded with silver nanoparticles were studied for conversion of 2,4-dinitrophenol (Kamal et al. 2017).

Cellulose is natural, most pervasive, renewable, and highly abundant organic polymer. It is non-toxic, colorless and odorless with auspicious qualities e.g. biocompatibility, thermal stability, hydrophilicity, excellent mechanical strength etc. however cellulose in its pure form has low or no adsorption capacity (Maneerung et al. 2008; Jia et al. 2012; Yang et al. 2012; Zhou et al. 2013; Haider et al. 2016).

The degradation of the dyes is well recognized reductive cleavage of azo group. Being a good electron donor, degradation reaction occurs on the surface of metal. The azo dyes molecules accept electrons from metal and transfer into transitional products when combining with H^+ (Li et al. 2015). Different reaction schemes and mechanism have been proposed and studied in this regard (Li et al. 2015; Ali et al. 2017; Khan et al. 2019). Proposed degradation mechanism is given below. (Fig. 1).

In this study degradation of some of the selected toxic dyes like 4-nitrophenol (4-NP) and various azo dyes (Congo Red (CR), Methylene Blue (MB), and Methyl orange (MO)) using zerovalent copper nanoparticles incorporated in MCC and functionalized MCC films has been studied. MCC was functionalized with the aim to eradicate dye effluents from wastewater. The acid and amino groups in functionalized MCC helps high uptake of Cu(II) ions possibly due to presence of more adsorption sites for metals ions and in binding dye molecules, thus improving adsorption process. Cu^{+2} form complex with matrix (MCC derivatives) by coordination bonds. The nanoparticles are retained in the composites as shown in (Fig. 2) because of metal and cellulose interaction.

Materials and methods

Materials

All chemicals and reagents, viz. Microcrystalline cellulose (MCC) (DAEJUNG 20–100 um), Nitric acid (HNO_3) (Sigma Aldrich), Phosphoric acid (H_3PO_4) (Sigma Aldrich), Sodium nitrite ($NaNO_2$) (Sigma Aldrich), Sulphuric acid (H_2SO_4) (Sigma Aldrich), Sodium hydroxide (NaOH) (Sigma Aldrich), p-Toluenesulfonyl chloride (TsCl) (DAEJUNG), Lithium Chloride Anhydrous (LiCl) (DAEJUNG), N,N-Dimethyl acetamide (DMAc) (Merck), Triethylamine (TEA), Hydrazinium hydroxide (Merck), Diethylamine (DEA) (DAEJUNG), Copper Sulphate (Sigma Aldrich), Sodium borohydride ($NaBH_4$) (Sigma Aldrich), Acetone (Merck), N,N-Dimethyl formamide

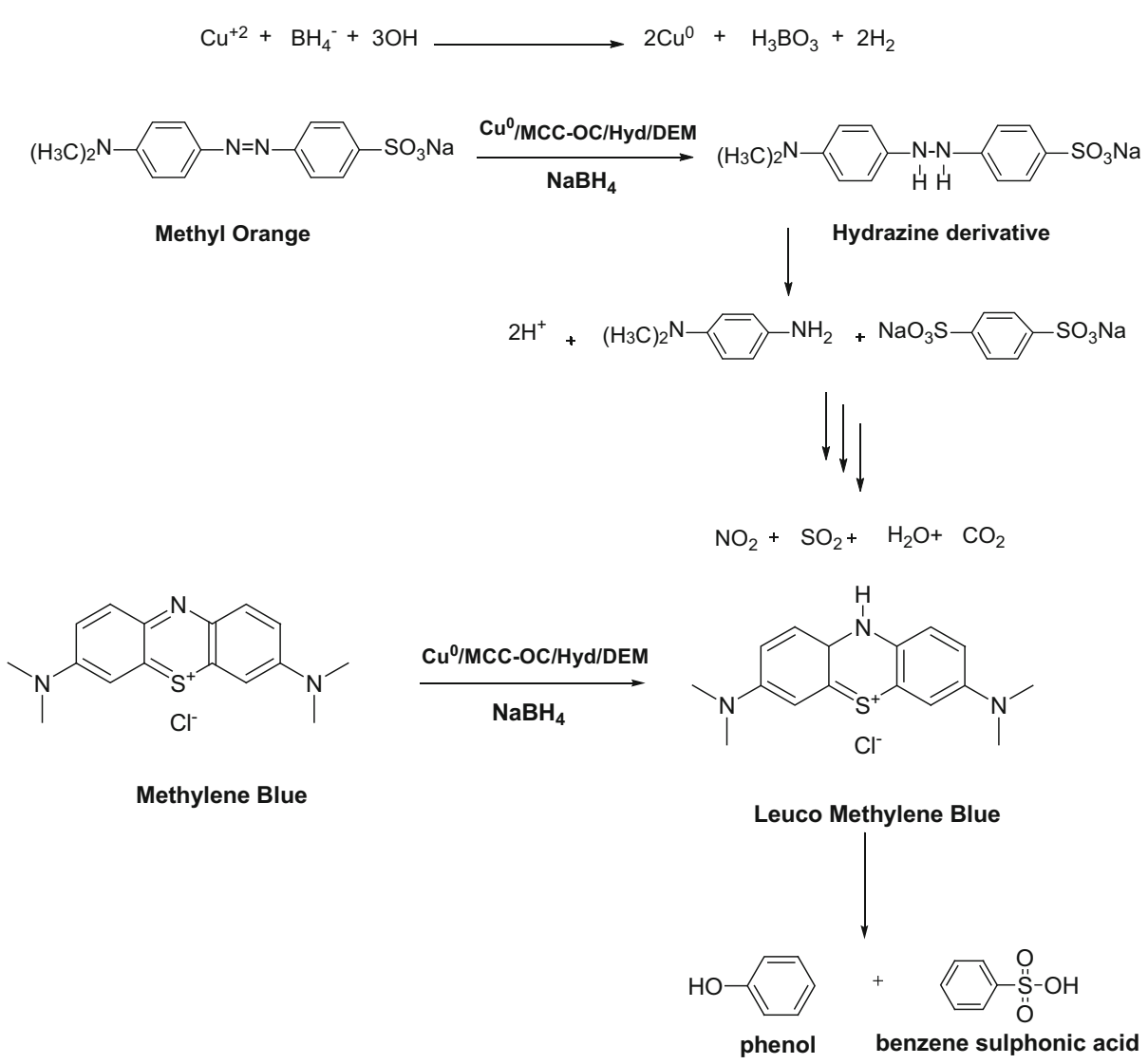

Fig. 1 Proposed degradation mechanism of Methyl orange and Methyl blue (Li et al. 2015; Ali et al. 2017)

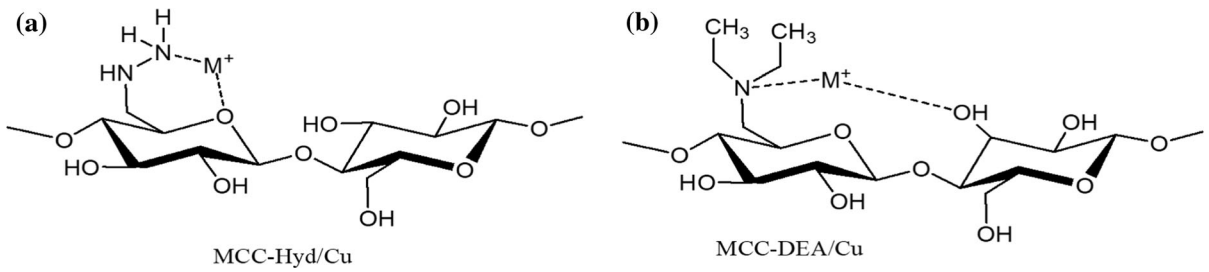

Fig. 2 Plausible complexation between metal ion and Ammino derivatives of cellulose

(DMF), Chloroform (Merck), Ethanol (Merck) and Deionized water (DI) (Sigma Aldrich) were procured from commercial sources as mentioned. All chemicals used for the synthesis and preparation of desired

catalysts and composites were of high purity and no further purification was needed.

Preparation of oxidized cellulose (OC)

Oxidized cellulose (OC) was synthesized by using acidic mixture and $NaNO_2$ as oxidizing agent. Mixture of Nitric acid and phosphoric acid were taken in 4:1 (v/v). To 70 mL solution of the acidic mixture, 5.0 g of MCC and 1.0 g of $NaNO_2$ was added simultaneously. An instantaneous creation of reddish-brown fumes occurred. The reaction was continued for 48 h at room temperature with occasional stirring. After 48 h the mixture seemed greenish in color. An excess of distilled water was added to the reaction mixture. The green color disappeared, and white fluffy solid was acquired. This mixture was filtered and washed several times with distilled water until the pH of filtrate become 4. Solid obtained was finally washed with acetone and dried in vacuum oven at 50 °C. (Kumar and Yang 2002). (Fig. 3).

Tosylation of microcrystalline cellulose

Tosylation of cellulose has been performed according to previously reported method (Rahn et al. 1996). Briefly, MCC (5.0 g, 30.8 mmol of glucose unit (French 2017) in 500 mL round bottom flask was kept in vacuum oven for drying at 70 °C, 120 mL of DMAc was added to it, and stirred at 120–130 °C for two hrs. It was then cooled to 100 °C and 10 g anhydrous LiCl in 25 mL of DMAc were added under stirring. The stirring was sustained overnight until complete dissolution of MCC. A transparent gel like solution formed which indicates complete dissolution.

In second step a mixture of TEA (18.6 ml, 185 mmol, 6 mol/AGU) in 10 mL DMAc was added to the gel like solution of MCC under energetic stirring at room temperature (RT), the stirring was sustained for another 30 min, followed by the drop wise addition of p-toluenesulfonyl chloride (35.3 g, 184.8 mmol, 6 mol/AGU) (dissolved in 25 mL of DMA) over a period of 30 min at 3–8 °C. The stirring was continued for another 24 h at RT, then the mixture was poured slowly in 1L of ethanol. Precipitation occurs, the precipitate was filtered off, and washed carefully with approximately 1L of distilled water. Precipitates were further washed with ethanol (250 mL) for three times to remove unreacted TsCl. The resulting TsMCC was kept in an oven at 50 °C for 48 h for drying. (Fig. 3).

Synthesis of 6-deoxycellulose amine derivatives

6-deoxycellulose amine derivatives of MCC were synthesized by replacing tosyl group with hydrazine and N,N-diethylamine by employing a method similar to previously reported method (Nazir and Iqbal 2020). 2 g of TsMCC was mixed with 20 mL of DMF in 100 mL round bottom flask at room temperature. The reaction mixture was allowed to react under stirring until the complete dissolution. Then addition of 10 mL hydrazine hydrate was done under stirring, the stirring was continued for another 2 h at RT and then the reaction mixture was refluxed at 80 °C for 24 h. orange color solution containing 6-Deoxycellulose hydrazide (MCC-Hyd) was obtained. This mixture was allowed to cool and then poured slowly into 250 mL of ethanol; formation of white precipitates occurred. This was then filtered and washed with ethanol thrice and dried at 50 °C under vacuum for 24 h.

Similar procedure was followed for the synthesis of 6-deoxycellulose(N,N-diethyl)amine (MCC-DEM) where N,N-Diethylamine was added in place of Hydrazine. (Fig. 3).

Preparation of MCC and modified MCC films

Composite films of cellulose and modified cellulose were prepared by mechanical mixing. Styrene–isoprene block copolymers (SIS) polymer was used as a binding agent to strengthen the films. 0.1 g SIS was dissolved in 20 mL of chloroform under continuous stirring at room temperature. 1 g MCC or its derivatives was dispersed in this mixture, stirring was continued for 1 h, after the complete dispersion the mixture was poured into petri dishes and left overnight for evaporation. Dried films were then peeled off and used further.

Preparation of copper nanoparticles

Copper nanoparticles were synthesized inside the layers of polymer films by uptake of Cu(II) ions followed by their reduction. Prepared films were dipped in 100 mL of 1 M $CuSO_4.7H_2O$ solution for adsorption of Cu(II) ions. Films were left in copper sulphate solution of 24 h to saturate the adsorption

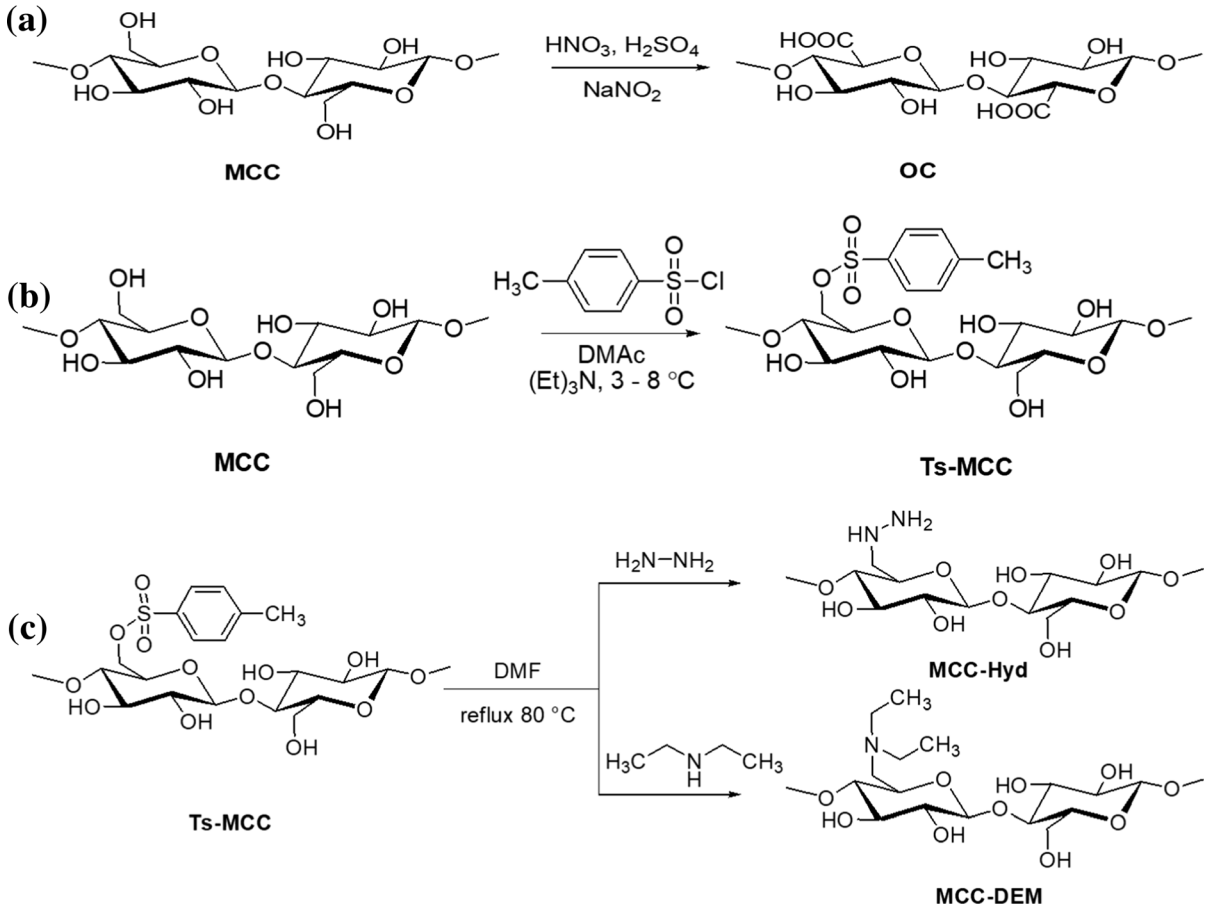

Fig. 3 Scheme of Synthesis of Microcrystalline Cellulose (MCC) Derivatives (**a**) MCC oxidation (**b**) synthesis of Ts-MCC (**c**) Amine functionalization of TS-MCC to MCC-Hyd and MCC-DEM

sites. After adsorption films were washed with D.I water and then kept in 50 mL of 0.5 M $NaBH_4$ solution to reduce Cu(II) ions to Cu^0 nanoparticles. After that Cu^0 embedded polymeric films were washed gently with deionized water and used freshly.

Catalytic reduction studies

The catalytic reduction studies were performed for 4-nitrophenol (4-NP) and various azo dyes (Congo Red (CR), Methylene Blue (MB), and Methyl orange (MO)) reductions using sodium borohydride. Quartz cuvette cell was used as reaction container. Solutions of 4-NP, dyes and sodium borohydride were prepared in D.I water with concentrations of 0.5 mM, 0.08 mM and 0.5 M respectively. 3 mL of 0.08 mM 4-Nitrophenol was taken in a cuvette cell to which 0.5 mL of 0.5 M freshly prepared $NaBH_4$ solution was added and its spectra on UV visible spectrophotometer was recorded. After that, Cu°-MCC strips were placed in this cuvette cell in such a position that UV light can easily pass through it. Reduction reaction was started as soon as the catalyst strips were placed in reaction vessel (cuvette) and absorption spectra was continuously recorded. The variations in absorbance value at 400 nm for 4-NP was plotted. For the reduction of other dyes (CR, MB, MO) same procedure was employed. Moreover, the degradation rate was also compared for each sample (catalyst) in the manner of percentage efficiency, which was calculated using following equation.

$$\%Efficiency = \left(\frac{A_0 - A_t}{A_0}\right)$$

where, A_0 is initial absorbance while A_t is absorbance at time t.

Characterization

Scanning electron microscope (SEM, JEOL JSM-7600f, Japan) was performed to find the morphology and presence of Cu-Nps over the surface of MCC and derived MCC films. Elemental analysis of modified MCC derivatives was conducted by elemental analyzer (CKIC 5E-CHNS-2200 and CKIC5E-IRS II ultimate analyzer). MCC and its derivatives were subjected to Powder XRD to confirm the crystal structure and homogeneity by using (diffractometer (D8 advance BRUKER, USA) in transmission mode° with Cu Kα radiation at voltage 40kv and current 20 mA. Samples were milled to form a fine powder (by using a mortar and pestle) before observing over a 2 theta range from 10° to 50°.The presence of Cu-Nps in films were further analyzed by XRD Using JEOL-JDX-II, X-ray diffractometer voltage 40kv and current 20 mA over a 2 theta range of 5° to 80°. The presence of Cu-Nps were further analyzed by XRD Using JEOL-JDX-II, X-ray diffractometer. XPS perkin-Elmer HI 5000 ESCA photo spectrometer using an Al Kα radiation at 14,866 eV in the range of 200 to 1400 eV was carried out for the confirmation of coper nanoparticles by elemental analysis. Bruker attenuated total reflectance Fourier transform infrared (ATR FT-IR) spectrophotometer (Bruker platinum ATR model Alpha spectrophotometer, Germany) in the range of 400–4000 cm^{-1} was used to perform FT-IR analysis. ^{1}HNMR spectra were recorded for all samples at room temperature in deuterated dimethyl sulfoxide (DMSO-d6) on a 400 MHz Bruker AV400 spectrometer (Bruker corporation MA, USA) with 64 scans for concentration of 20 mg/mL^{-1}. The reduction in dyes concentration with the passage of time was evaluated via (Thermo-scientific evolution-300) UV/VIS spectrophotometer.

Results and discussion

FTIR analysis

The FT-IR spectra of MCC and prepared derivatives is shown in Fig. 4. Examination of MCC showed a broad absorption band at 3325 cm^{-1} for –OH stretching. –OH, bending was observed at 1372 cm^{-1} while –CH bending was at 1236 cm^{-1} and C-O stretching at 1024 cm^{-1} corresponds to glycosidic linkage in the

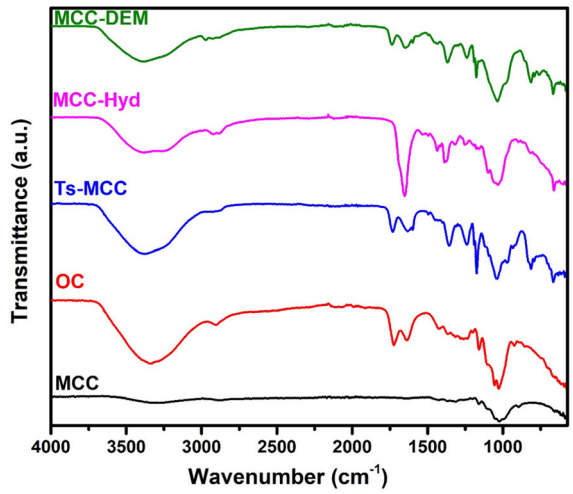

Fig. 4 FTIR spectra of pure MCC and its derivatives, OC, Ts-MCC, MCC-Hyd, and MCC-DEM

structure of cellulose (Nazir et al. 2021). Peaks allocated were well assigned and extensively described in previous literature (Singha and Guleria 2014; Haider et al. 2016; Kenawy et al. 2018).(Fig. 4a). Spectrum of oxidized cellulose showed a strong absorption band at 1728 cm^{-1} corresponds to the presence of carbonyl stretching, confirms the presence of acidic group (oxidation) (Fig. 4b). FT-IR analysis of tosylated cellulose (Fig. 4c) showed additional band of $–SO_2$ asymmetric stretch at 1355 cm^{-1}. A band of $–SO_2$ symmetric stretch is observed at 1175 cm^{-1}. At 815 cm^{-1} the band observed corresponds to -S–O–C stretching vibrations proving successful substitution (Rahn et al. 1996; Schmidt et al. 2014). After the reaction with hydrazine hydrate in MCC-Hyd, the additional bands appeared at 3384 cm^{-1} and 3240 cm^{-1} for N–H Stretch and at 1337 cm^{-1} corresponds to C–N stretching vibration in the spectrum justifies that surface is functionalized with hydrazine hydrate (Fig. 4d). Following absorption bands has been observed for MCC-DEM, a strong absorption band at 3384 cm^{-1} for –OH stretch, -CH stretch at 2976 cm^{-1}, 1373 cm^{-1}, and 1464 cm^{-1} for $–CH_2$ and $–CH_3$ bending, respectively. The strong band at 1361 cm^{-1} confirms the presence of –C-N stretch (Fig. 4e).

[1]HNMR analysis

[1]H-NMR spectroscopy was used to obtain the information about the local environment of the proton in the MCC and its derivatives shown in Fig. 5. Pristine MCC peaks appear between 3–5.5 ppm (Guan et al. 2015). In [1]HNMR of OC chemical shift values appeared downfield around 12.58 ppm is justified by the close vicinity of highly electronegative oxygen atom. In [1]HNMR of Ts-MCC benzene ring proton appeared at 7.75 CH, 7.35 CH ppm while methyl group CH_3 appears at 2.42 ppm (Heinze, Pfeifer et al. 2016, Nazir and Iqbal 2020). For MCC-Hyd single NH appeared as a sharp signal at 6.2 ppm while NH_2 protons expected to appear at 3.23 ppm was masked under MCC backbone peaks. In case of MCC-DEM there was no peak for NH observed, suggesting the bonding occurred between Nitrogen and methylene of MCC. DEA CH_2 multiplet and CH_3 triplet appeared at 2.59 and 1.15 ppm, respectively (Nazir and Iqbal 2020). [1]H-NMR of MCC derivatives is in good agreement with the relevant FTIR results.

Elemental analysis

Elemental analysis (CHNS analysis) was useful in obtaining the degree of substitution by finding out the percentage of the elements found in the sample. Sulfur analysis of tosylated cellulose (Ts-MCC) was used to find degree of tosylation, which was found to be 42%

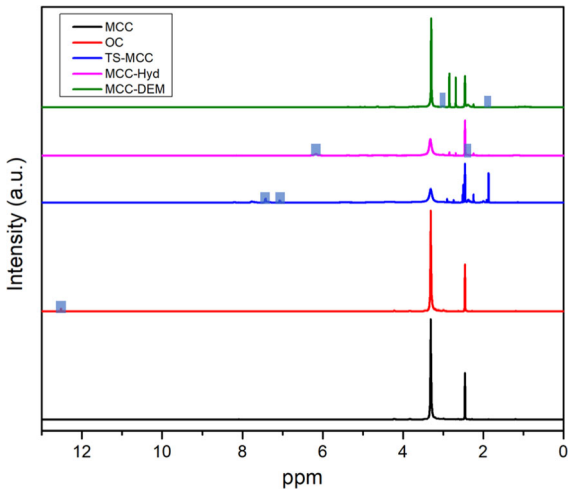

Fig. 5 [1]HNMR spectra of OC, Ts-MCC, MCC-Hyd and MCC-DEM

based on Sulfur analysis. Nitrogen analysis was carried out for the MCC-Hyd and MCC-DEM. Degree of amination was found to be 0.40 to 0.43, suggesting that the maximum number of tosyl group has been removed. Elemental analysis data in Table 1 proved that there is no chlorine moiety resulting from a side product. No polymer degradation resulted in the synthesis reaction. Yield of the reactions was more than 80%. In all the derivatives, a trace amount of sulfur of 0.5% and 1.01% for MCC-Hyd and MCC-DEM was found, respectively. Complete elimination of Tosyl group was not possible due to the polymeric structure of the cellulose, but Nitrogen content of 12.26% and 5.43% was found in case of MCC-Hyd, MCC-DEM, respectively. Results revealed that upon substitution with amino groups a considerable amount of nitrogen content was observed which indicates the successful preparation of both the derivatives.

XRD analysis

The XRD pattern of MCC, OC, MCC-Hyd, and MCC-DEM are shown in Fig. 6. To investigate the effect of cellulose modification by the amine groups, the crystal structure of the cellulose and its aminated cellulose derivatives were analyzed with wide angle powder X-ray diffractogram shown in Fig. 6. The XRD pattern showed that MCC and OC are cellulose I while the MCC-Hyd and MCC-DEM samples are not well crystallized and grown in amorphous form (Gericke et al. 2012; French and Santiago Cintrón 2013; French 2014; Ali et al. 2017, Ismail, Gul et al. 2019). The cellulosic diffraction pattern altered as stated in previous studies (El-Sayed, El-Sakhawy et al. 2018) after the. Tosylation and modification with amine groups indicating that all the chemical modification of cellulose (Gupta et al. 2013) in LiCl/DMA mixture affected the lattice structure and altered the crystallinity of the cellulose as appeared from reasonable lowering of the peak intensity. Ts-MCC displayed a broad peak at $2\theta = 20$ (110) of amorphous.

cellulose II. Samples that have been fully dissolved and then crystallized are usually found in the cellulose II form, if they don't, then, they are amorphous. (Mittal et al. 2011; El-Sayed et al. 2018a, b; French 2020).

Figure 7 graph (a, b, c, and d) displays the XRD analysis of copper nanoparticle embedded films of MCC, OC, MCC-Hyd, and MCC-DEM respectively.

Table 1 Elemental (CHNS) analysis of synthesized cellulose derivatives

Sr. No	Sample Code	Carbon % (Found)	Hydrogen % (Found)	Nitrogen % (Found)	Sulfur % (Found)
1	MCC-Hyd	38.93	6.53	12.26	–
2	MCC-DEM	47.44	6.43	5.43	–
3	Ts–MCC	31.34	4.16	–	4.49

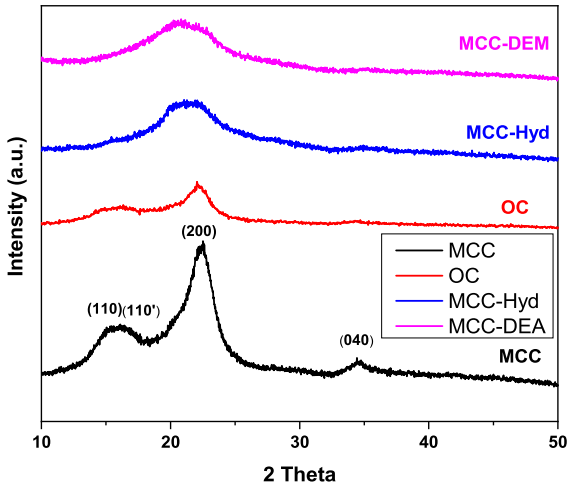

Fig. 6 XRD pattern of pure MCC, OC, MCC-Hyd and MCC-DEM

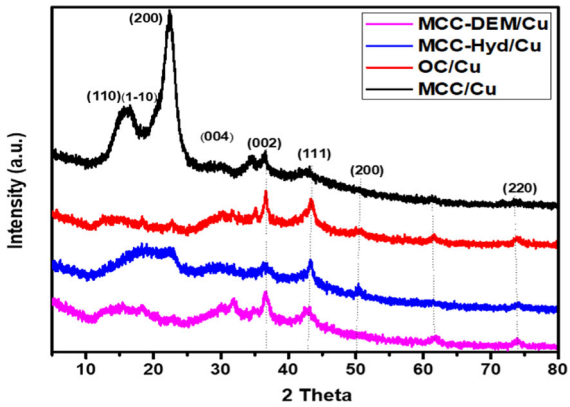

Fig. 7 XRD Pattern of pure MCC, OC, MCC-Hyd, and MCC-DEM with embedded Cu nanoparticles

All patterns show additional peaks at 2θ 43.2° (111), 50.3° (200) and 73.9° (220) (JCPDS no 89–2838) that are the distinctive diffraction peaks belonging to copper nanoparticles. Some additional peaks at 2θ 36.4°, 42.2°, 61.3° and 73.5° corresponding to JCPDS no 05–0667 were also observed in these spectra. These may occur due to the formation of copper oxide because copper is readily oxidized to CuO and Cu_2O. Modified cellulose derivatives (OC, MCC-Hyd, and MCC-DEM) showed low crystallinity (Park et al. 2010) with characteristic near amorphous form (Demircan and Zhang 2017) as illustrated in Fig. 7 graph (b, c, and d). The decrease in crystallinity of derivatives from original microcrystalline cellulose during modification is due to the disturbance of inter and intramolecular chains of cellulose structure. As these samples had been dissolved completely before being derivatized, (homogeneous reaction), so that all molecules would be statistically similar. Therefore, these samples are amorphous. While OC samples would expect to only have substituents on the crystal surface, the reagents would not penetrate the crystal internal molecules, (heterogenous reaction) so the original cellulose I structure could be retained.

XPS analysis

The oxidation state and compositional analysis of copper nanoparticles has been investigated using XPS. The complete XPS spectrum of copper nanoparticles from 200 to 1400 eV are illustrated in Fig. 8a, b. Oxidation state of copper was observed in reduced form. The prepared catalyst clearly indicates C 1 s, O 1 s, Cu 2p 3/2 and Cu 2P 1/2 peaks, revealing the successful preparation of copper nanoparticles. The peak at 281.5 corresponds to C 1 s, while peak at 532.6 indicates the presence of O 1 s.the high resolution of oxygen peak is due to the presence of C–O–C group in cellulose structure, and also might be due to the oxide formation. As Cu^0 in NPs form may readily oxidized to Cu(I) or Cu(II) by the presence of atmosphere oxygen. The observed at 932.2 eV and 951.4 attributes to Cu 2p 3/2 and Cu 2P ½ respectively.

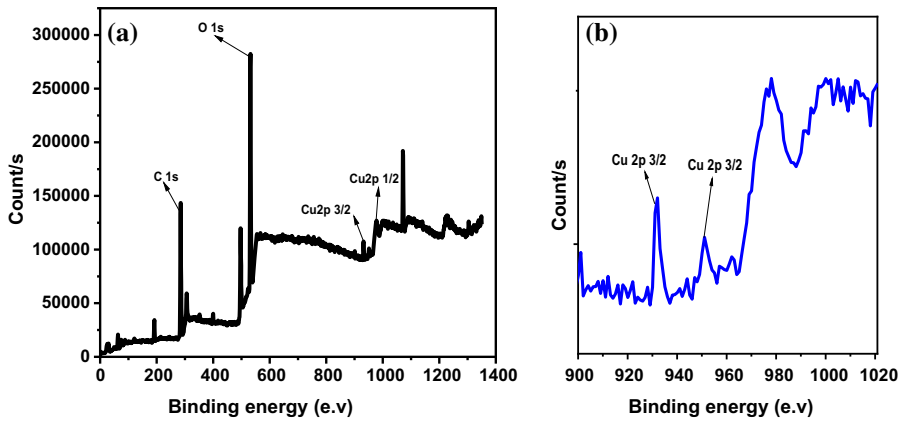

Fig. 8 **a** Complete **XPS** spectrum of Cu nanoparticles from 0 to 1400 eV. **b** Cu 2p 3/2 and Cu 2p ½ spectral line peaks of copper nanoparticles

SEM analysis

Figure 9 shows SEM images of films from pure MCC and its derivatives with and without Cu NPs. Pure MCC has homogeneous structure while the derivatives have an interconnected heterogeneous structure. The unmodified MCC show mutually connected fibrous network having high and smooth surface area. In case of films having MCC and its derivatives embedded with the Cu NPs presence of small granules confirms that Cu NPs successfully templated in the MCC and its derivatives with the polymer support. Figure 9c shows large aggregates. Agglomeration occurs because of van der Waals interaction, which results in decrease of surface area and hence reduction in catalytic activity. Many attempts were taken to improve the efficiency of zero-valent metals nanoparticles catalytic reduction. Acoustic cavitation appears to deagglomerate particles and improve mass transfer through the collapse of cavities or microbubbles (Chand et al. 2009) (Segura et al. 2012) (Pinjari et al. 2013) Acoustic cavitation, hydrodynamic cavitation, and water jet cavitation was used in different studies to reduce agglomeration. (Gogate et al. 2013) (Sivakumar and Pandit 2002, Gogate and Pandit 2005, Hutli, Nedeljkovic et al. 2013) Feng & Dongye modified conventional method by using water soluble starch as a stabilizer for the synthesis of pallaized iron (Fe-Pd) bimetallic nanoparticles. The starched nanoparticles showed much less agglomeration than those prepared without stabilizer (He, Zhao et al. 2005). Another and most widely used method is to use "catalyst support". It can be either inorganic or organic. Organic supports are better than inorganic as they have a few advantages such as they can be easily functionalized and chemical inertness

Fig. 9 SEM Images of films of MCC and its derivatives **(a)** ▶ MCC, **(b)** OC, **(c)** MCC-Hyd, **(d)** MCC-DEM, a') MCC with Cu NPs (b') OC with Cu NPs (c') MCC-Hyd with Cu NPs (d') MCC-Hyd with Cu NPs. Red arrows show Cu NP s embedded in MCC and its derivatives in polymer films; Scale bar is 1um

i.e., they do not interfere with the catalyst (Guo, Liu et al. 2014). In this study we have selected cellulose as a support material because of natural abundance, environmental benign and low cost. Cellulose have been modified to acid and amine groups for the better loading of nanoparticles(Dong, Miller et al. 2012).

we have prepared round films of diameter approx. 6 cm and cut them into small strips of size $0.5cm^{2-} \times 1cm^2$. We have obtained good results for all the dyes with this sample, so the strip/ part of film that we used in degradation experiment must not have aggregates. Aggregates that have been observed in SEM image might be in the particular part of film that has been analyzed under SEM.

Degradation studies

Degradation experiments were carried out on 4NP, CR, MB, and MO dye. For this purpose, a stock solution of 0.5 mM for 4NP and 0.1 mM for dyes (CR, MB, and MO) was made which was further diluted up to 0.05 Mm and 0.08 Mm for 4NP and dyes, respectively. Degradation studies were carried out for all the prepared samples. For all catalysts $0.5cm^2 \times 1cm^2$ strips, 2.5 mL of aqueous solution of dyes and 0.5 mL of $NaBH_4$ solution was used(Konstantinou and Albanis 2004; Haider et al. 2016). Reaction was

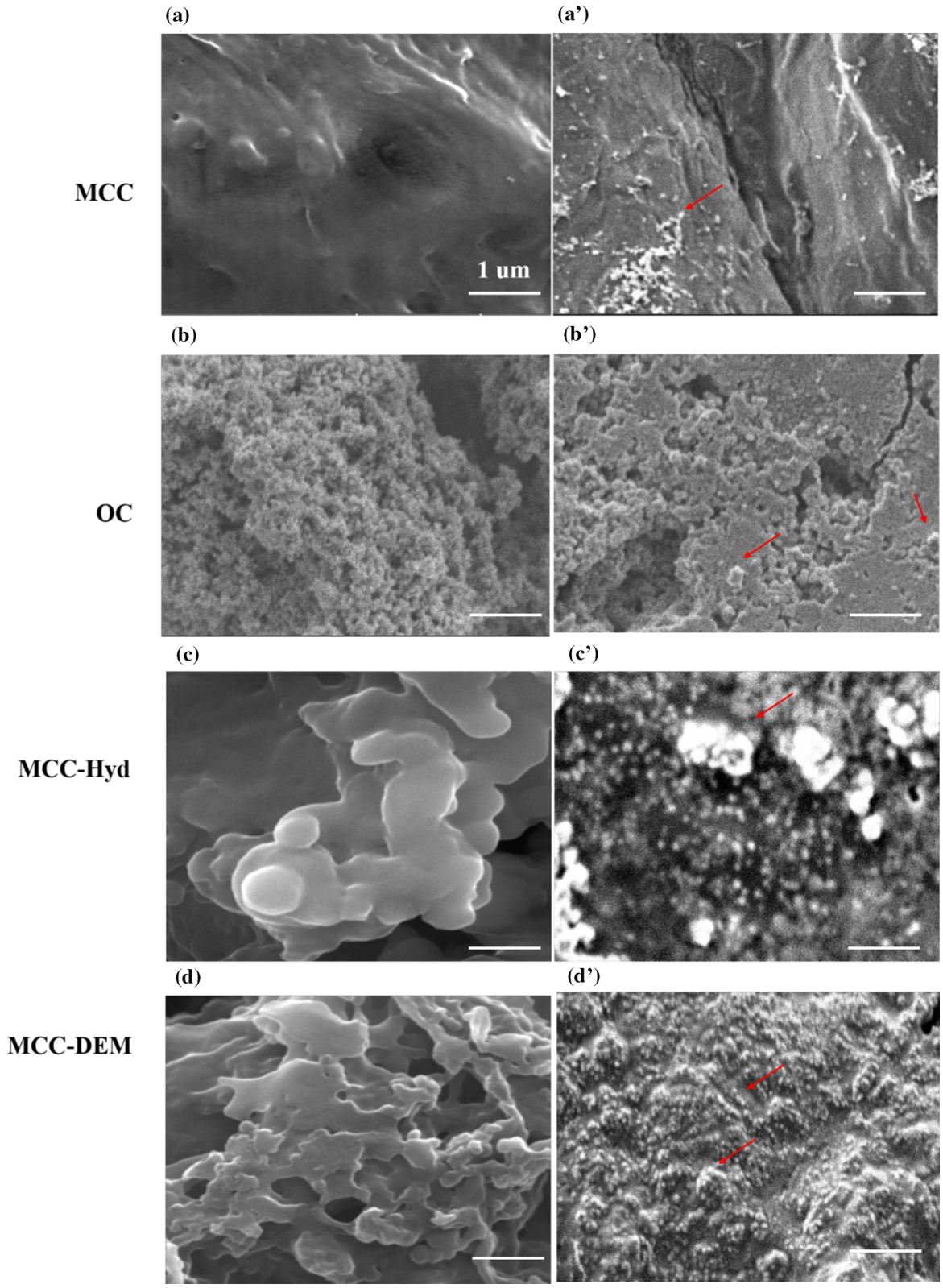
(a)
(a')
MCC
1 um
(b)
(b')
OC
(c)
(c')
MCC-Hyd
(d)
(d')
MCC-DEM

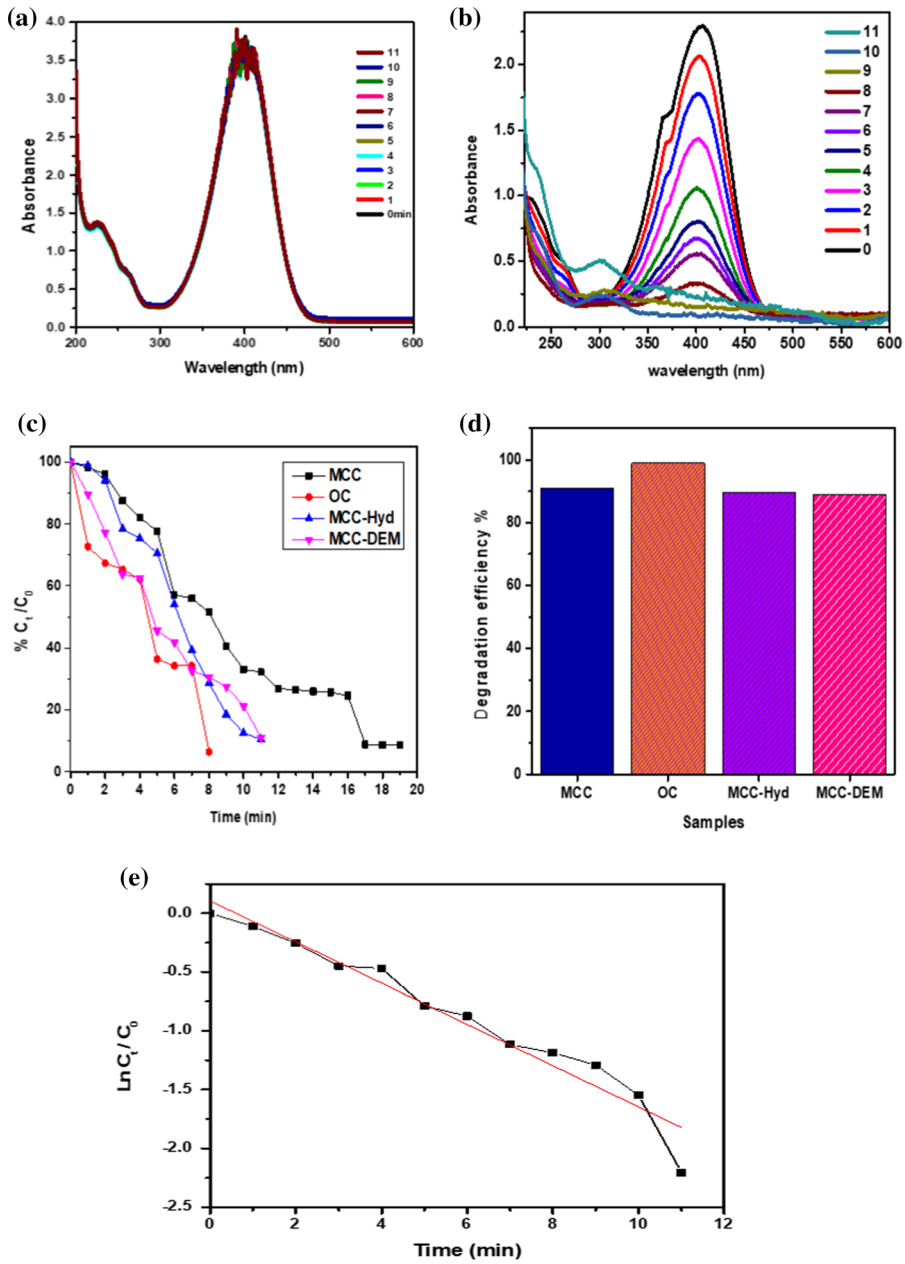

Fig. 10 Absorption spectra of 4-NP at different interval of time. **(a)** Bare MCC-DEM film. **(b)** Cu-MCC-DEM film. **(c)** Activity of all prepared films incorporated with Cu^0 Nps against 4-NP degradation **(d)** degradation efficiency of all films loaded with Cu^0 Nps against 4-NP degradation. **(e)** Reaction kinetics obtained as a result of Ln C_t/C_0. Experimental conditions: 0.08 Mm 2.5 mL of 4-NP, 0.5 mL $NaBH_4$ 0.5 M, 1 cm strip of each film

carried out in quartz cuvette cell and spectra was recorded on spectrophotometer.

First bare MCC-DEM film was placed in UV cuvette containing 2.5 mL of aqueous solution of 4NP and 0.5 mL of $NaBH_4$ and its spectra was recorded every minute until half an hour. The typical peak of 4-NP absorbance appeared at λ_{max} 310 nm, which shifted to 400 nm by the addition of $NaBH_4$ solution, reason behind is extended conjugation. Figure 10(a) shows that no change in absorbance intensity at 400 nm was observed (Haider et al. 2016; Ali et al. 2017). Which shows the poor catalytic performance of

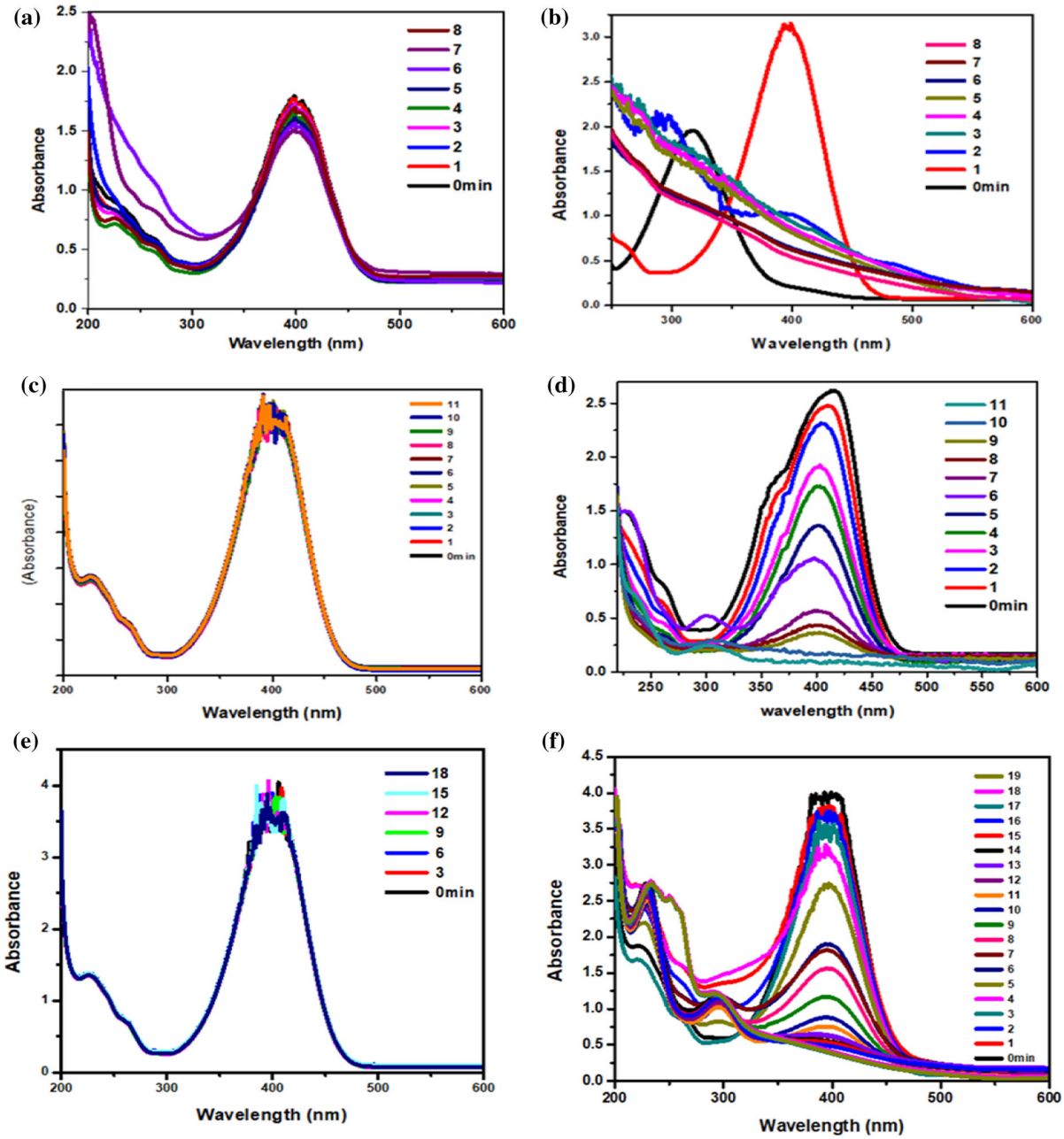

Fig. 11 Absorption Spectra of 4-NP aqueous solution at different interval of time. **(a)** Bare OC film **(b)** Cu^0-OC film. **(c)** Bare MCC-HYD film **(d)** Cu^0- MCC-HYD film. (e) Bare MCC film. (f) Cu^0-MCC film. Experimental conditions: 0.05 Mm 2.5 mL of 4-CR, 0.5 mL $NaBH_4$ 0.5 M, 1 cm strip of each film

bare MCC-DEM film towards the reduction of 4NP. The reduction of 4np in absence of suitable catalyst is difficult to achieve due to the high kinetic barrier between phenolate ions ($C_6H_4NO^{3-}$) and borate ions (BH^{4-}).

After that under similar conditions Cu^0 loaded, strip was introduced to the cuvette containing reaction mixture. Change in color of 4NP was observed, it starts disappearing as soon as the Cu^0 strip was introduced. Figure 10(b) shows that absorbance intensity of peak at 400 nm progressively decreases and

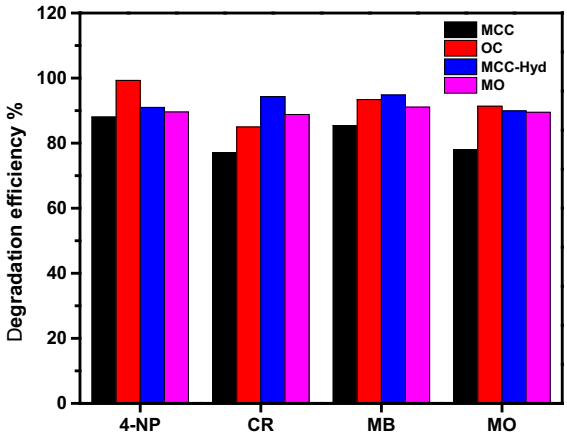

Fig. 12 Comparison percentage efficiencies of all the samples against all dyes

completely disappeared after 19mints, show excellent catalytic reduction of 4NP by Cu^0 loaded MCC-DEM film as compared to previous studies (Ali et al. 2017). Figure 10(c) illustrate the activity of all the prepared samples in the presence of ZVC NPs against degradation of 4-NP with the passage of time in terms of $\%C_t / C_o$. It is clear from figure that all samples incorporated with Cu^0 show excellent efficiency, but highest efficiency was observed with Cu-OC in minimum time. Figure 10(d) shows percentage degradation efficiency of all prepared Cu^0 loaded films against 4-NP degradation. All ZVC NPs loaded films show excellent degradation efficiency, highest efficiency achieved for 4-NP was 99%. Previously 75% conversion of 4NP occurred in 12 min with Cu/CS-CMM (Haider et al. 2016). The natural log ($\ln C_t/C_0$) of the absorption peak at λ_{max} 400 nm Vs time indicating a large linear portion. This validates that reaction proceeds with pseudo first order kinetics. The rates of reaction were 1.30×10^{-1}, 1.75×10^{-1}, 2.17×10^{-1} and 2.53×10^{-1} min^{-1} for Cu-MCC, Cu-MCC-DEM, Cu-MCC-Hyd, and Cu-OC respectively.

Figure 11(a–f) illustrates the absorption spectra of 4-NP with bare OC, Cu^0-OC, bare MCC-Hyd, Cu^0-MCC-Hyd, bare MCC and Cu^0-MCC films respectively. OC readily degrade 4NP the absorption peak disappears in only 8 min, while MCC-Hyd takes 11 min to degrade 4NP. Unmodified MCC takes bit longer then modified MCC derivatives, the absorption peak of 4NP with Cu^0-MCC diminished in 19 min. This shows low efficiency of Cu^0-MCC as compared to modified MCC derivatives, reason could be the low adsorption of metal ions by MCC. in both case the deration of 4NP is much better and faster than with other materials as reported previously. (Zhao, Mele et al. 2010).

Figure 13 graph (b) depict gradual decrease in absorbance at wavelength 498 nm after every minute. Cu^0-MCC-DEM takes 10 min to degrade CR to 88.8%. Figure 13(c) illustrate the activity of all the prepared samples against degradation of CR with the passage of time in terms of C_t / C_o. It is clear from figure that all samples showed excellent efficiency, but highest efficiency was observed with Cu^0-MCC-Hyd in minimum time of 8 min. Figure 13(d) shows percentage degradation efficiency of all prepared films against CR degradation. All ZVC NPs loaded films show excellent degradation efficiency, highest efficiency achieved for CR degradation was 94.2% with MCC-Hyd film in the presence of ZVC NPs. The graph obtained as a result of $\ln C_t/C_0$ Vs time suggest that degradation reaction of CR in the presence of ZVC NPs proceeds with pseudo first order kinetics. The rates of reactions were 2.37×10^{-1}, 2.53×10^{-1}, 2.78×10^{-1} and 1.81×10^{-1} min^{-1} for Cu-MCC,

Table 2 Summary of Degradation Results with different Dyes

Sample	4-NP		CR		MB		MO	
	% Degradation	Time (min)	% Degradation	Time (min)	% Degradation	Time (min)	% Degradation	Time (min)
MCC	88	19	77	11	85.4	10	77.9	12
OC	99	8	85	10	93.4	9	91.3	10
MCC-Hyd	91	11	94.2	8	94.8	11	89.9	11
MCC-DEM	89.6	12	88.8	10	91	13	89.5	10

Cu-MCC-DEM, Cu-MCC-Hyd, and Cu-OC respectively.

Figure 14 shows degradation spectra of methylene blue with amino modified cellulose MCC-DEM. Cu^0-MCC-DEM (Fig. 12b) takes 13 min to degrade MB to 91%. CR takes minimum time of 9 min and maximum of 13 min to show its catalytic activity (Fig. 14c). Highest degradation efficiency of 94.8% has been observed with Cu^o- MCC-Hyd films in 11 min (Fig. 14d) which was better than reported somewhere(Kono 2017, Ng and Leo 2019). Reaction kinetic was found to be pseudo first order (Fig. 14e). Reaction rates obtained for Cu-MCC, Cu-MCC-DEM, Cu-MCC-Hyd and Cu-OC were 1.25×10^{-1}, 1.56×10^{-1}, 2.68×10^{-1} and 3.36×10^{-1} min^{-1} respectively.

Similarly, Fig. 15 shows degradation spectra of methyl orange with MCC-DEM with and without nanoparticles. No change in absorbance occurred in the absence of zero valent nanoparticles (Fig. 15a) while decrease in absorbance at λ_{max} 464 nm with the passage of time was observed with Cu^0 loaded MCC-DEM film (Fig. 15b). Cu^o-MCC-DEM Shows catalytic activity in 10 min (Fig. 15c). Figure 12d shows degradation of all prepared films incorporated with ZVC in terms of percentage efficiency. Highest efficiency of 89.9% has been observed for MO, which is more than previously reported study(Li et al. 2015). Linearity of graph ln C_t/C_0 Vs. time depict pseudo-first order kinetics and rate of reactions were 1.95×10^{-1}, 1.81×10^{-1}, 1.89×10^{-1} and 2.2×10^{-1} min^{-1} for Cu-MCC, Cu-MCC-DEM, Cu-MCC-Hyd and Cu-OC respectively.

Figure 12 illustrates the percentage efficiencies of all the samples for all four dyes. Graphs shows that Modified cellulose showed excellent degradation efficiency for all dyes. Oxidized cellulose showed highest efficiency in almost all cases. While amino modified derivatives also exhibit more than 85% efficiency in all cases. Which depicts the effectiveness of as prepared samples against dye degradation. The percent degradation of all the dyes and required time for it are summarized in Table 2 as well.

Conclusion

In summary, carboxylic acid and amino functionalized cellulose derivatives viz. oxidized cellulose (OC), 6-Deoxycellulosehydrazide (MCC-Hyd) and 6-deoxycellulose(N,N-diethyl) amine (MCC-DEM) were successfully synthesized. FT-IR, CHNS and NMR analysis confirmed the synthesis of derivates. As prepared derivatives were employed for uptake of copper ions from aqueous solution for the very first time. Films of cellulose and modified cellulose was successfully prepared and used as support materials for zero valent copper nanoparticles. Zero valent copper nanoparticles were prepared via a chemical reduction method. OC, MCC-Hyd and MCC-DEM showed excellent degradation efficiency in the presence of Cu^0 nanoparticles. In most the of cases amino modified cellulose showed highest degradation efficiency probably due to larger uptake of Cu(II) ions because of the presence of more adsorption sites (NH_2 groups) which fix the metal ion in polymer matrix by dipole-ion interactions and electrostatic forces. Considering the simple preparation method and sustainable support material, the prepared derivatives can also be used for uptake of other heavy metal ions for the purpose of catalyzing the degradation of organic pollutants and their removal from wastewater.

Acknowledgments The authors thank School of Natural Sciences (SNS), National University of Sciences and Technology (NUST), for providing all facilities for the completion of the project.

Funding This research received no external funding.

Declarations

Conflicts of interest The authors declare to have no conflicts of interest.

Human and animal rights The research does not involve any Human or Animal and informed consent is not applicable in this case.

References

Ali F, Khan SB, Kamal T, Alamry KA, Asiri AM, Sobahi TR (2017) Chitosan coated cotton cloth supported zero-valent nanoparticles: simple but economically viable, efficient and easily retrievable catalysts. Sci Rep 7(1):1–16. https://doi.org/10.1038/s41598-017-16815-2

Ali N, Kamal T, Ul Islam M, Khan A, Shah SJ, Zada A (2018) Chitosan coated cotton cloth supported copper nanoparticles for toxic dye reduction. Int J biolog macromolec.

111:832–838. https://doi.org/10.1016/j.ijbiomac.cxx2018.01.092

Amoozegar MA, Hajighasemi M, Hamedi J, Asad S, Ventosa A (2011) Azo dye decolorization by halophilic and halotolerant microorganisms. Annals of Microbiol 61(2):217–230. https://doi.org/10.1007/s13213-010-0144-y

Bakhsh EM, Khan SA, Marwani HM, Danish EY, Asiri AM, Khan SB (2018) Performance of cellulose acetate-ferric oxide nanocomposite supported metal catalysts toward the reduction of environmental pollutants. Int J Biol Macromol 107:668–677. https://doi.org/10.1016/j.ijbiomac.2017.09.034

Chen Q, Luo Z, Hills C, Xue G, Tyrer M (2009) Precipitation of heavy metals from wastewater using simulated flue gas: sequent additions of fly ash, lime and carbon dioxide. Water Res 43(10):2605–2614. https://doi.org/10.1016/j.watres.2009.03.007

Chand R, Ince NH, Gogate PR, Bremner DHJS, Technology P (2009) Phenol degradation using 20, 300 and 520 kHz ultrasonic reactors with hydrogen peroxide, ozone and zero valent metals. 67(1):103–109. https://doi.org/10.1016/j.seppur.2009.03.035

Da browskiHubickiPodkościelny AZP, Robens E (2004) Selective removal of the heavy metal ions from waters and industrial wastewaters by ion-exchange method. Chemosphere 56(2):91–106. https://doi.org/10.1016/j.chemosphere.2004.03.006

Demircan D, Zhang B (2017) Facile synthesis of novel soluble cellulose-grafted hyperbranched polymers as potential natural antimicrobial materials. Carbohyd Polym 157:1913–1921. https://doi.org/10.1016/j.carbpol.2016.11.076

Dong B, Miller DL, Li CYJTjopcl, (2012) Polymer single crystal as magnetically recoverable support for nanocatalysts. J 3(10):1346–1350. https://doi.org/10.1021/jz300434c

El-Sayed NS, Abd El-Aziz M, Kamel S, Turky G (2018a) Synthesis and characterization of polyaniline/tosylcellulose stearate composites as promising semiconducting materials. Synth Met 236:44–53. https://doi.org/10.1016/j.synthmet.2018.01.001

El-Sayed NS, El-Sakhawy M, Brun N, Hesemann P, Kamel S (2018) New approach for immobilization of 3-aminopropyltrimethoxysilane and TiO2 nanoparticles into cellulose for BJ1 skin cells proliferation. Carbohydr polym. 199:193–204. https://doi.org/10.1016/j.carbpol.2018.07.004

French AD (2014) Idealized powder diffraction patterns for cellulose polymorphs. Cellulose 21(2):885–896. https://doi.org/10.1007/s10570-013-0030-4

French AD (2020) Increment in evolution of cellulose crystallinity analysis. Springer. https://doi.org/10.1007/s10570-020-03172-z

French AD, Santiago Cintrón MS (2013) Cellulose polymorphy, crystallite size, and the segal crystallinity index. Cellulose 20(1):583–588. https://doi.org/10.1007/s10570-012-9833-y

Gericke M, Schaller J, Liebert T, Fardim P, Meister F, Heinze T (2012) Studies on the tosylation of cellulose in mixtures of ionic liquids and a co-solvent. Carbohyd Polym 89(2):526–536. https://doi.org/10.1016/j.carbpol.2012.03.040

Gogate PR, Bhosale GS (2013) Comparison of effectiveness of acoustic andhydrodynamic cavitation in combined treatment schemes for degradation of dye wastewaters. Chemical Engineering and Processing: Process Intensification 71: 59-69.https://doi.org/10.1016/j.cep.2013.03.001

Gogate, PR, Pandit ABJUs (2005) A review and assessment of hydrodynamic cavitation as a technology for the future. Ultrasonics Sonochemistry 12(1–2): 21–27. https://doi.org/10.1016/j.ultsonch.2004.03.007

Guan Y, Chen J, Qi X, Chen G, Peng F, Sun R (2015) Fabrication of biopolymer hydrogel containing Ag nanoparticles for antibacterial property. Ind Eng Chem Res 54(30):7393–7400. https://doi.org/10.1021/acs.iecr.5b01532

Guo Z, Liang X, Pereira T, Scaffaro R, Hahn HT (2007) CuO nanoparticle filled vinyl-ester resin nanocomposites: Fabrication, characterization and property analysis. Compos Sci and Technol. 67(10):2036–2044. https://doi.org/10.1016/j.compscitech.2006.11.017

Guo Z, Liu B, Zhang Q, Deng W, Wang Y, Yang YJCSR (2014) Recent advances in heterogeneous selective oxidation catalysis for sustainable chemistry. Chemical Society Reviews 43(10):3480–3524. https://doi.org/10.1039/C3CS60282F

Gupta P, Uniyal V, Naithani S (2013) Polymorphic transformation of cellulose I to cellulose II by alkali pretreatment and urea as an additive. Carbohyd Polym 94(2):843–849. https://doi.org/10.1016/j.carbpol.2013.02.012

Haider S, Kamal T, Khan SB, Omer M, Haider A, Khan FU, Asiri AM (2016) Natural polymers supported copper nanoparticles for pollutants degradation. Appl Surf Sci 387:1154–1161. https://doi.org/10.1016/j.apsusc.2016.06.133

Haines A, Kovats RS, Campbell-Lendrum D, Corvalán C (2006) Climate change and human health: impacts, vulnerability and public health. Public Health 120(7):585–596. https://doi.org/10.1016/j.puhe.2006.01.002

He F, Zhao DJEs (2005) Preparation and characterization of a new class of starch-stabilized bimetallic nanoparticles for degradation of chlorinated hydrocarbons in water. Environmental Science & Technology 39(9): 3314–3320. https://doi.org/10.1021/es048743y

Heinze T, Pfeifer A, Koschella A, Schaller J, Meister F (2016) Solvent-free synthesis of 6-deoxy-6-(ω-aminoalkyl) amino cellulose. J Appl Polym Sci. https://doi.org/10.1002/app.43987

Hutli EAF, Nedeljkovic MS, Radovic NAJP (2013) Nano-and micro-scale surface modification of FCC metal using high submerged cavitating water jet. Plasmonics 8(2):843–849. https://doi.org/10.1007/s11468-013-9481-6

Ismail M, Gul S, Khan M, Khan MA, Asiri AM, Khan SB (2019) Green synthesis of zerovalent copper nanoparticles for efficient reduction of toxic azo dyes congo red and methyl orange. Green process and synthesis 8(1):135–143. https://doi.org/10.1515/gps-2018-0038

Jia B, Mei Y, Cheng L, Zhou J, Zhang L (2012) Preparation of copper nanoparticles coated cellulose films with antibacterial properties through one-step reduction. ACS Appl

Mater Interfaces 4(6):2897–2902. https://doi.org/10.1021/am3007609
Kamal T, Anwar Y, Khan SB, Chani MTS, Asiri AM (2016a) Dye adsorption and bactericidal properties of TiO2/chitosan coating layer. Carbohyd Polym 148:153–160. https://doi.org/10.1016/j.carbpol.2016.04.042
Kamal T, Khan SB, Asiri AM (2016b) Synthesis of zero-valent Cu nanoparticles in the chitosan coating layer on cellulose microfibers: evaluation of azo dyes catalytic reduction. Cellulose 23(3):1911–1923. https://doi.org/10.1007/s10570-016-0919-9
Kamal T, Ahmad I, Khan SB, Asiri AM (2017) Synthesis and catalytic properties of silver nanoparticles supported on porous cellulose acetate sheets and wet-spun fibers. Carbohyd Polym 157:294–302. https://doi.org/10.1016/j.carbpol.2016.09.078
Kenawy I, Hafez M, Ismail M, Hashem M (2018) Adsorption of Cu (II), Cd (II), Hg (II), Pb (II) and Zn (II) from aqueous single metal solutions by guanyl-modified cellulose. Int J Biol Macromol 107:1538–1549. https://doi.org/10.1016/j.ijbiomac.2017.10.017
Khan SA, Khan SB, Farooq A, Asiri AM (2019) A facile synthesis of CuAg nanoparticles on highly porous ZnO/carbon black-cellulose acetate sheets for nitroarene and azo dyes reduction/degradation. Int J Biol Macromol 130:288–299. https://doi.org/10.1016/j.ijbiomac.2019.02.114
Konstantinou IK, Albanis TA (2004) TiO2-assisted photocatalytic degradation of azo dyes in aqueous solution: kinetic and mechanistic investigations: a review. Appl Catal B 49(1):1–14. https://doi.org/10.1016/j.apcatb.2003.11.010
Kumar V, Yang T (2002) HNO3/H3PO4–NaNO2 mediated oxidation of cellulose-preparation and characterization of bioabsorbable oxidized celluloses in high yields and with different levels of oxidation. Carbohyd Polym 48(4):403–412. https://doi.org/10.1016/S0144-8617(01)00290-9
Li P, Song Y, Wang S, Tao Z, Yu S, Liu Y (2015) Enhanced decolorization of methyl orange using zero-valent copper nanoparticles under assistance of hydrodynamic cavitation. Ultrason Sonochem 22:132–138. https://doi.org/10.1016/j.ultsonch.2014.05.025
Maneerung T, Tokura S, Rujiravanit R (2008) Impregnation of silver nanoparticles into bacterial cellulose for antimicrobial wound dressing. Carbohyd Polym 72(1):43–51. https://doi.org/10.1016/j.carbpol.2007.07.025
Min M, Shen L, Hong G, Zhu M, Zhang Y, Wang X, Chen Y, Hsiao BS (2012) Micro-nano structure poly (ether sulfones)/poly (ethyleneimine) nanofibrous affinity membranes for adsorption of anionic dyes and heavy metal ions in aqueous solution. Chem Eng J 197:88–100. https://doi.org/10.1016/j.cej.2012.05.021
Mittal A, Katahira R, Himmel ME, Johnson DK (2011) Effects of alkaline or liquid-ammonia treatment on crystalline cellulose: changes in crystalline structure and effects on enzymatic digestibility. Biotechnol Biofuels 4(1):1–16. https://doi.org/10.1186/1754-6834-4-41
Nazir F, Iqbal M (2020) Synthesis, characterization and cytotoxicity studies of aminated microcrystalline cellulose derivatives against melanoma and breast cancer cell lines. Polymers 12(11):2634. https://doi.org/10.3390/polym12112634
Nazir F, Ashraf I, Iqbal M, Ahmad T, Anjum S (2021) 6-deoxy-aminocellulose derivatives embedded soft gelatin methacryloyl (GelMA) hydrogels for improved wound healing applications: In vitro and in vivo studies. Int J Biol Macromol. https://doi.org/10.1016/j.ijbiomac.2021.06.112
Pal S, Patra AS, Ghorai S, Sarkar AK, Das R, Sarkar S (2015) Modified guar gum/SiO 2: development and application of a novel hybrid nanocomposite as a flocculant for the treatment of wastewater. Environ Sci: Water Res Technol 1(1):84–95. https://doi.org/10.1039/C4EW00023D
Park S, Baker JO, Himmel ME, Parilla PA, Johnson DK (2010) Cellulose crystallinity index: measurement techniques and their impact on interpreting cellulase performance. Biotechnol Biofuels 3(1):1–10. https://doi.org/10.1186/1754-6834-3-10
Parshetti G, Telke A, Kalyani D, Govindwar SP (2010) Decolorization and detoxification of sulfonated azo dye methyl orange by Kocuria rosea MTCC 1532. J Hazard Mater 176(1–3):503–509. https://doi.org/10.1016/j.jhazmat.2009.11.058
Pinjari D, Prasad K, Gogate P, Mhaske S, Pandit AJCE, Intensification PP (2013) Intensification of synthesis of zirconium dioxide using ultrasound: effect of amplitude variation. Chemical Engineering and Processing: Process Intensification 74:178–186. https://doi.org/10.1016/j.cep.2013.09.010
Raaschou-Nielsen O, Andersen ZJ, Beelen R, Samoli E, Stafoggia M, Weinmayr G, Hoffmann B, Fischer P, Nieuwenhuijsen MJ, Brunekreef B (2013) Air pollution and lung cancer incidence in 17 European cohorts: prospective analyses from the European Study of cohorts for air pollution effects (ESCAPE). Lancet Oncol 14(9):813–822. https://doi.org/10.1016/S1470-2045(13)70279-1
Rahn K, Diamantoglou M, Klemm D, Berghmans H, Heinze T (1996) Homogeneous synthesis of cellulose p-toluenesulfonates in N, N-dimethylacetamide/LiCl solvent system die Angewandte Makromolekulare Chemie. Appl Macromolec Chem and Phys 238(1):143–163. https://doi.org/10.1002/apmc.1996.052380113
Razali M, Kim JF, Attfield M, Budd PM, Drioli E, Lee YM, Szekely G (2015) Sustainable wastewater treatment and recycling in membrane manufacturing. Green Chem 17(12):5196–5205. https://doi.org/10.1039/C5GC01937K
Robinson T, McMullan G, Marchant R, Nigam P (2001) Remediation of dyes in textile effluent: a critical review on current treatment technologies with a proposed alternative. Biores Technol 77(3):247–255. https://doi.org/10.1016/S0960-8524(00)00080-8
Schmidt S, Liebert T, Heinze T (2014) Synthesis of soluble cellulose tosylates in an eco-friendly medium. Green Chem 16(4):1941–1946. https://doi.org/10.1039/C3GC41994K
Segura Y, Martínez F, Melero JA, Molina R, Chand R, Bremner DHJACBE (2012) Enhancement of the advanced Fenton process (Fe0/H2O2) by ultrasound for the mineralization of phenol. Applied Catalysis B: Environmental 113:100–106. https://doi.org/10.1016/j.apcatb.2011.11.024
Sha Y, Mathew I, Cui Q, Clay M, Gao F, Zhang XJ, Gu Z (2016) Rapid degradation of azo dye methyl orange using hollow cobalt nanoparticles. Chemosphere 144:1530–1535
Shokouhimehr M (2015) Magnetically separable and sustainable nanostructured catalysts for heterogeneous reduction

of nitroaromatics. Catalysts 5(2):534–560. https://doi.org/10.1016/j.chemosphere.2015.10.040

Singha A, Guleria A (2014) Chemical modification of cellulosic biopolymer and its use in removal of heavy metal ions from wastewater. Int J Biol Macromol 67:409–417. https://doi.org/10.1016/j.ijbiomac.2014.03.046

Sivakumar M, Pandit ABJUs (2002) Wastewater treatment: a novel energy efficient hydrodynamic cavitational technique. 9(3):123–131. https://doi.org/10.1016/S1350-4177(01)00122-5

Spadaro JT, Isabelle L, Renganathan V (1994) Hydroxyl radical mediated degradation of azo dyes: evidence for benzene generation. Environ Sci Technol 28(7):1389–1393. https://doi.org/10.1021/es00056a031

Teh CY, Budiman PM, Shak KPY, Wu TY (2016) Recent advancement of coagulation–flocculation and its application in wastewater treatment. Ind Eng Chem Res 55(16):4363–4389. https://doi.org/10.1021/acs.iecr.5b04703

Wang J, Gu H (2015) Novel metal nanomaterials and their catalytic applications. Molecules 20(9):17070–17092. https://doi.org/10.3390/molecules200917070

Wang KP, Lin SB, Wang NN, Ke AR (2012) A novel gold nanoparticle/poly (AMPS-co-HEMA) composite hydrogel for selective catalysis. Adv Mater Res, Trans Tech Publ. https://doi.org/10.4028/www.scientific.net/AMR.399-401.704

Wang P, Lin Z, Su X, Tang Z (2017) Application of Au based nanomaterials in analytical science. Nano Today 12:64–97. https://doi.org/10.1016/j.nantod.2016.12.009

Yang G, Xie J, Hong F, Cao Z, Yang X (2012) Antimicrobial activity of silver nanoparticle impregnated bacterial cellulose membrane: effect of fermentation carbon sources of bacterial cellulose. Carbohyd Polym 87(1):839–845. https://doi.org/10.1016/j.carbpol.2011.08.079

Yang J, Yu J-H, Strickler JR, Chang W-J, Gunasekaran S (2013) Nickel nanoparticle–chitosan-reduced graphene oxide-modified screen-printed electrodes for enzyme-free glucose sensing in portable microfluidic devices. Biosens Bioelectron 47:530–538. https://doi.org/10.1016/j.bios.2013.03.051

Youssef NA, Shaban SA, Ibrahim FA, Mahmoud AS (2016) Degradation of methyl orange using Fenton catalytic reaction. Egypt J Pet 25(3):317–321. https://doi.org/10.1016/j.ejpe.2015.07.017

Zhou Z, Lu C, Wu X, Zhang X (2013) Cellulose nanocrystals as a novel support for CuO nanoparticles catalysts: facile synthesis and their application to 4-nitrophenol reduction. RSC Adv 3(48):26066–26073. https://doi.org/10.1039/c3ra43006e